Fractal dimension analysis of periapical reactive bone in response to root canal treatment

Yen-Yun Yu, MS,[a] Hsieh Chen, BS,[b] Chi-Hao Lin, PhD,[c] Chung-Ming Chen, PhD,[d] Tina Oviir, DDS,[e] Ssu-Kuang Chen, DDS, MSD, PhD,[f] Lars Hollender, DDS, PhD,[f] Taipei, Taiwan
NATIONAL TAIWAN UNIVERSITY, TSING HUA UNIVERSITY, AND UNIVERSITY OF WASHINGTON

Objective. Mathematical morphology and box counting were used to extract trabecular pattern and to evaluate changes of reactive bone following root canal treatment.
Study design. Periapical radiographs were digitized and processed with mathematical morphology operations known as skeletonization. The trabecular patterns resulting from this skeletonization process were further analyzed with fractal dimension (FD) analysis using the box-counting method. Two groups of regions of interest (ROI) were selected from 19 subjects for the analysis.
Results. Seventeen patients in one group and 13 patients in the other showed decreased FD in the reactive bone region after clinically successful root canal treatment (RCT). Significant changes in FD were noted 6 months after RCT ($P < .05$). Kappa analysis indicated significant reproducibility between the 2 groups of ROIs.
Conclusions. Mathematical morphology combined with box counting showed decrease of FD in reactive bone regions after clinically successful endodontic treatment. **(Oral Surg Oral Med Oral Pathol Oral Radiol Endod 2008;xx:xxx)**

Periapical reactive bone formation, commonly called condensing osteitis or focal sclerosing osteitis, is associated with teeth having infected vital or necrotic pulps, and is a common radiographic finding.[1] Reactive bone formation is often confused with idiopathic bone formation such as bony islands, idiopathic osteoscleroris, and enostosis. Reactive bone formation in the jaws is most commonly caused by odontogenic infections including those related to inflammation or necrosis of the dental pulp and is typically found adjacent to the apical parts of the root, with or without an accompanying widened periodontal ligament space or periapical radiolucent lesion. There are few studies on the fate of reactive bone formation following root canal treatment. It has been reported that if the cause of inflammation is eliminated, the reactive bone seems to regress or disappear.[1-2]

Bone texture analysis provides information about bone structures in a noninvasive manner. Mathematical morphology image processing is one method that has been shown useful for bone texture analysis.[3-7] The use of FD to describe the structure of trabecular bone has been described.[8-14] There are 2 widely used definitions of FD: the Hausdorff dimension and the box-counting dimension. The Hausdorff dimension has significant theoretical interest, but it is the box-counting dimension that is usually used to determine experimental values.[15] The box-counting algorithm was used to quantify the trabecular pattern by analyzing the trabecular bone and bone marrow interface. It assesses the fractal dimension of the connectivity of the trabecular boundary. A higher fractal dimension indicates a more complex structure. The aim of the study was to see if significant changes of the bony structures of reactive bone following endodontic treatment could be demonstrated by the mathematical morphology and box-counting methods. We hypothesized that fractal dimension of reactive bone formation decreases after successful root canal treatment (RCT).

MATERIAL AND METHODS

This study was approved by the Human Subjects Review Committee and Radiographic Safety Committee of the University of Washington. The patients were selected from the referrals to the Endodontic Depart-

Support for this study was received from the National Science Council, Taiwan.
[a]Research assistant, Institute of Biomedical Engineering, College of Medicine and Engineering, National Taiwan University, Taipei, Taiwan.
[b]Research assistant, Department of Materials Science and Engineering, College of Engineering, National Tsing Hua University.
[c]Research assistant, Department of Civil Engineering, College of Engineering, National Taiwan University, Taipei, Taiwan.
[d]Professor, Institute of Biomedical Engineering, College of Medicine and Engineering, National Taiwan University. Taipei, Taiwan.
[e]Clinical Associate Professor, Department of Endodontics, University of Washington, Seattle, WA.
[f]Professor, Division of Oral Radiology, Department of Oral Medicine, School of Dentistry, University of Washington, Seattle, WA.
Received for publication Jul 15, 2007; returned for revision Mar 22, 2008; accepted for publication May 27, 2008.
1079-2104/$ - see front matter

doi:10.1016/j.tripleo.2008.05.047

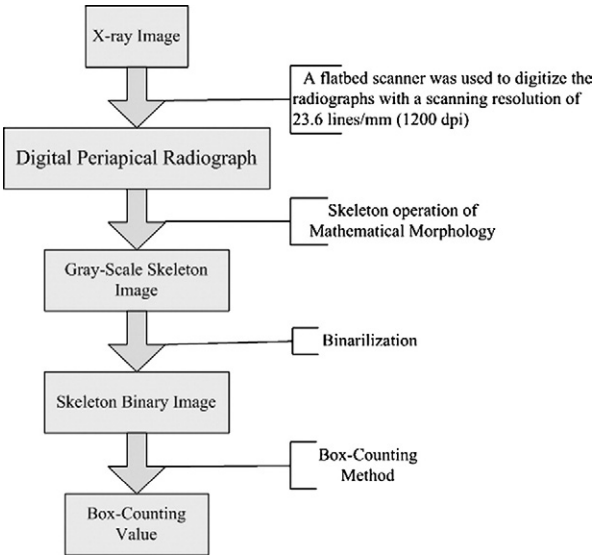

Fig. 1. Flow diagram of this study.

ment for conventional RCT. The study included patients 18 years and older, with radiographically visible periapical radiolucent lesions more than 2 mm in diameter that were associated with necrotic maxillary or mandibular posterior teeth. Forty patients volunteered to participate in the study. Each subject had 1 posterior tooth with a periapical lesion that needed RCT. Of these 40 individuals, 19 were followed for 6 months. These 19 cases were used for analysis in this study.

Endodontic treatment was completed in 1 or 2 sittings by undergraduate and/or graduate students at the Endodontic Department of the dental school. If more than one sitting was needed to complete the RCT, calcium hydroxide paste was placed in the root canals under a temporary filling (Fig. 1).

Radiographic procedure

Periapical radiographs were made within a week before RCT, and all 19 subjects had follow-up radiographs taken 6 months after RCT. All radiographs were taken with a standardized method, using an aiming device (DSR, EMS, Richardson, TX) to facilitate reproducible projection geometry and Kodak Insight F-Speed film (Eastman Kodak Co, Rochester, NY). All radiographic exposures were made using the same x-ray unit (Schick, CDR Discovery; Schick Technology Inc, Long Island City, NY) operating at 60 kV, 8 mA, and 0.4-s exposure time. Radiographs were developed with standardized conditions using an automated processor (Dent-X 810 Basic, Dent-X Corp. USA, Elmsford, NY) and Kodak RP X OMATIC solutions. A flatbed scanner (Epson Expression 636, Epson America, Inc, Torrance, CA) with transparency unit was used to digitize the radiographs using a scanning resolution of 23.6 lp/mm (1200 DPI, [dots per inch]).

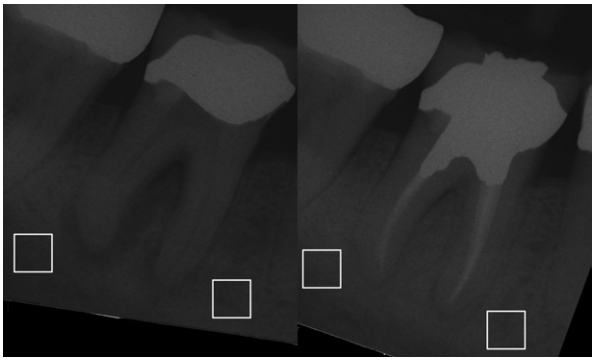

Fig. 2. Periapical radiographs showing the regions of interest (*white squares*). Left image is before RCT and the right image after RCT.

Selection of regions of interest

After rotational adjustments of the digital images to align roots in serial images for all cases, 2 pairs of ROIs were selected around the periapical lesions for each patient, as decided independently and jointly by 2 observers. The size of all ROIs was 128 × 128 pixels, with a pixel size of 0.02 mm (Fig. 2). This study used only pretreatment and 6-month post-treatment radiographs for analysis.

Mathematical morphology operation

A 7 × 7-pixel disk-shape structuring element was used to extract the binary skeletal pattern from gray-scale x-ray images. The skeleton operation equation was:

$$SK = \bigcup_{n=0}^{N} Sn(x) = \bigcup_{n=0}^{N} [(X \Theta nB) - (X \Theta nB) \circ B] \quad (1)$$

where X = original image, SK = sumset of images of skeleton operation, Sn(x) = subset image of skeleton operation, n = operation sequence number, N = ending operation number, U = union, and B = structuring element.

The skeletal patterns were extracted by the morphologic operation (Θ = erosion and $\circ$ = opening) on original images with the structuring elements. The skeletal pattern images of sumset n = 1-5 were extracted for quantitative evaluation. However, this process did not remove any noise when the number of operations was zero (n = 0). A threshold level of 1, the lowest possible, was used to retain the greatest detail of the skeletal pattern.[4] On a processed skeletal binary image, the skeletal structure reveals the pattern of trabecular

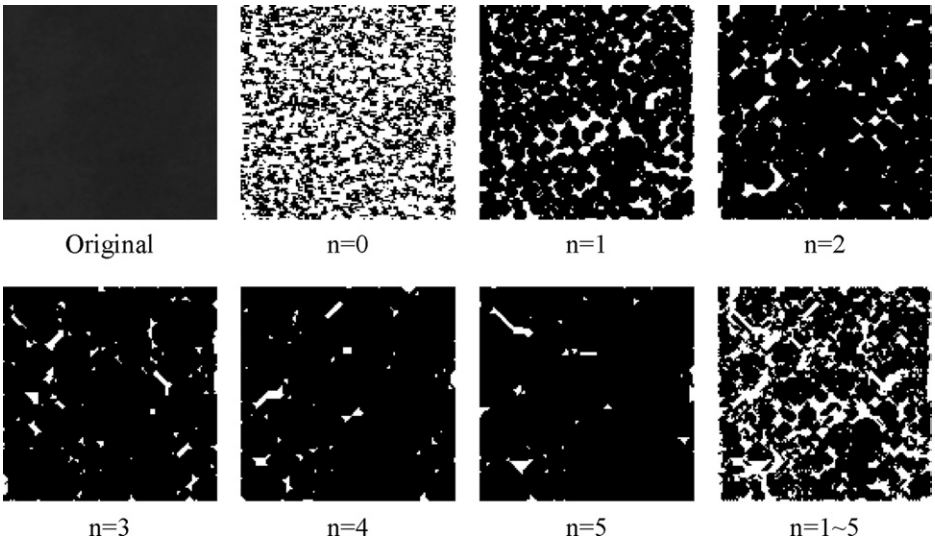

Fig. 3. Series of morphologically processed subset periapical images including the original image, the processed image with different iterations (n = 0, 1 . . . 5), and the sumset image (n = 1-5).

bone and the nonskeletal structure displays a pattern that represents the bone marrow space (Fig. 3).[5]

Box counting

The box-counting technique depended on identifying the boundary of trabecular bone and marrow. After mathematical morphology operations, the skeletonized image was covered with boxes of varying sizes (e). Square boxes with widths of 2, 4, 8, and 15 pixels were used. The number of boxes N(e) containing the boundary points was counted. The procedure was repeated for varying box sizes, and the statistical behavior of the features of size e was mapped over a range of scales. Then N(e) was plotted as a function of e on a log-log plot. The box counting was determined as the negative slope of the linear regression of the curve (Fig. 4).

Data analysis

All statistical analyses were performed with SPSS software (SPSS Inc., Chicago, IL). Nonparametric Wilcoxon signed rank test, as well as 2-tailed Z tests of significance were used. Kappa analysis was used to quantify the reproducibility of 2 groups of ROIs.

RESULTS

Double logarithmic plots of the counted number of boxes versus the sizes of boxes showed a good approximation to a straight line in all cases. The images of the trabecular bone showed fractal behavior. Seventeen of 19 patients showed decreased fractal dimension in the reactive bone formation area in the first group of ROIs and 13 in the second group. Significant changes of fractal dimension, calculated by mathematical morphology operations combined with box counting, could be noted 6 months after RCT (Table I, $P = .005$ and 0.048). The Kappa analyses indicate significant reproducibility between the first and second groups of ROIs (Table II, $\kappa = 0.406$ and $P = .028$).

DISCUSSION

This study demonstrated that fractal dimension of reactive bone decreases significantly 6 months after successful RCT. This is consistent with the hypothesis that the dense reactive bone would change toward a more normal density after successful RCT. The teeth in this study had been studied to disclose early bone formation after endodontic treatment of teeth with radiolucent periapical lesions.[16] All of these teeth showed signs of healing at the 6-month recall, corroborating the findings of a decrease in reactive bone found in our study.

Two groups of ROIs were selected for double determinations. Kappa analysis showed that the reproducibility was significant ($P = .028$), and the κ value indicated good reproducibility ($\kappa = 0.406$).[17] The repeated measurements showed consistency with the initial measurements. In 4 cases the fractal dimensions increased or decreased slightly in the reactive bone regions. This could be explained by the possibility that in these cases remodeling of reactive bone progressed at a slower rate. Another possibility is that the factors causing the reactive bone formation had not been completely removed by RCT in these cases.[18]

In this study the images were digitized by a flatbed

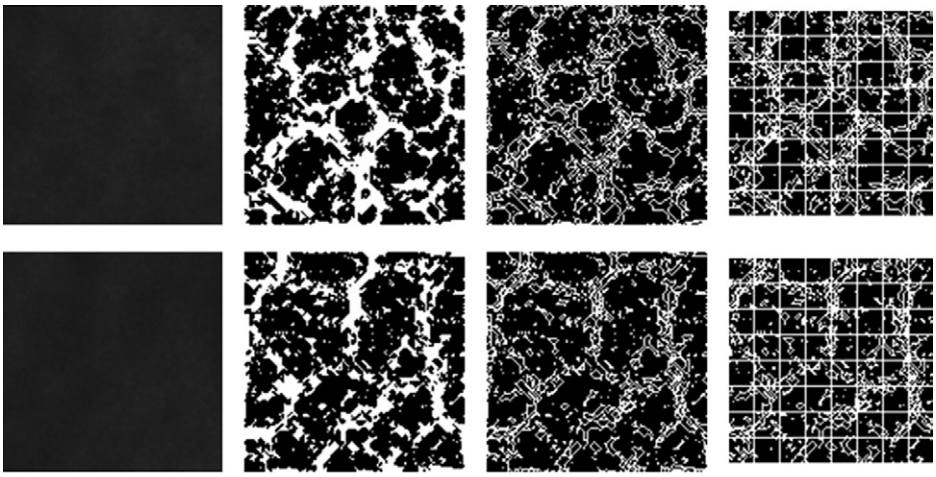

Fig. 4. Diagrammatic representation of procedure in this study, Selected ROIs from digitized periapical radiograph (**A**), skeletonized binary image after mathematic morphology operation and thresholiding (**B**), and trabecular bone and bone marrow interface (**C**). The boxes of varying sizes are applied to the boundary (**D**) and the number of boundary-containing squares is counted for each box size. Upper row is the pretreatment and the lower row is the post-treatment.

Table I. Reactive bone texture variables statistically different before and after root canal treatment

	Group 1		*Group 2*	
Case no.	*FD Pretreatment*	*FD Post-treatment*	*FD Pretreatment*	*FD Post-treatment*
1	1.672	1.670	1.750	1.720
2	1.562	1.561	1.568	1.559
3	1.625	1.657	1.789	1.803
4	1.610	1.536	1.607	1.549
5	1.577	1.650	1.616	1.702
6	1.740	1.704	1.692	1.704
7	1.617	1.520	1.563	1.511
8	1.653	1.606	1.577	1.549
9	1.699	1.636	1.670	1.648
10	1.613	1.596	1.594	1.565
11	1.585	1.548	1.609	1.650
12	1.730	1.702	1.726	1.681
13	1.571	1.528	1.553	1.561
14	1.590	1.551	1.632	1.641
15	1.575	1.550	1.699	1.682
16	1.573	1.547	1.612	1.549
17	1.747	1.722	1.768	1.711
18	1.724	1.708	1.715	1.707
19	1.722	1.623	1.728	1.580
	$P = .005$		$P = .048$	

FD, fractal dimension.

scanner. There is some loss of image information in the digitization process[19]; however, the major concern of inhomogeneity in the scanning process should have a limited effect on the results. Differences in image density should have limited effects on mathematical morphology processing. A high spatial resolution of about 0.02-mm pixel width was used for the digitization. The 128 × 128-pixel ROI covers a 2.56-mm-square area. This was aimed at limiting the selected area to reactive bone formation and to avoid including radiolucent areas. The effects of image spatial resolution and the size of the ROI, along with the area selected, remain to be studied.

It was difficult to find an exact threshold value for extracting bone structure. Selection of a high threshold

Table II. Reactive bone formation at 2 groups of regions of interest

		Group 2		
		+	−	*Total*
Group1	+	2	0	2
	−	4	13	17
Total		6	13	19

$\kappa = 0.406$.
$P = .028$.
+, fractal dimension increased after RCT; −, fractal dimension decreased after RCT.

value can result in excluding skeletal elements with low pixel intensity. A low threshold value may include the marrow spaces, as bony structures might be regarded as skeletal. The threshold method cannot separate trabecular bone from other tissues with high pixel value. Hence, we used the skeleton method, which has been applied to the extraction of the characteristic pattern of trabecular bone in digital images to overcome these limitations. In the skeleton operation based on mathematical morphology, the most local maximums of image, which represent trabecular pattern, can be filtered efficiently by using a gray-scale histogram. Thus, it is possible to recognize trabecular pattern as separate from the background, the intensity of which became zero after applying the skeleton method. Zero can then be categorically used as a threshold value to separate trabecular pattern from other tissues.

In skeleton processing, a 7 × 7-pixel disk-shaped structuring element was used based on trabecular width.[20] The operation sequence number with a higher number of operations (n) caused more skeletal elements to disappear from the high frequency area. With a lower number of operations (n), more detail can be preserved. The skeletal pattern images of sumset n = 1-5 were extracted for quantitative evaluation. After skeleton processing, the edge information of each image was broken and, thus, cannot be used directly in the box-counting processing. This study extracted only the center 120 × 120-pixel part of each image for analysis depending on the diameter of structure element being 7 pixels. Square boxes with a width of 2, 4, 8, and 15 pixels were used because they were all factors of 120 and had almost the same horizontal interval between each of the 2 variables in a log-log plot.[21,22] All parameters were designed carefully in accordance with the above theory.

Generally, mathematical morphology can overcome exposure problems well. A realistic variation in the amount of radiation between exposures is not considered a limiting factor, based on Beer's law,[23] as the images should result in the same trabecular pattern. In theory, this method does not require the images to be acquired from the same projection angle. However, further studies need to be conducted to confirm these assumptions.

CONCLUSION

This study demonstrated that fractal dimension of reactive bone decreases significantly after successful root canal treatment. It is consistent with the hypothesis presented that the dense reactive bone changes toward a normal density after successful root canal treatment.

The method used was a combination of mathematical morphology and box counting. There have been no previous reports to quantitatively evaluate the change of reactive bone formation associated with teeth having necrotic pulps and periapical lesions following endodontic treatment. The method described and used in this study might be a useful quantitative method for determining changes in bony structures of the jaws.

REFERENCES

1. Hedin M, Polhagen L. Follow-up study of periradicular bone condensation. Scand J Dent Res 1971;79:436-40.
2. Geraets WG, Van der Stelt PF, Netelenbos CJ, Elders PJ. A new method for automatic recognition of the radiographic trabecular pattern. J Bone Miner Res 1990; 5:227-33.
3. Cortet B, Dubois P, Boutry N, Bourel P, Cotton A, Marchandise X. Image analysis of the distal radius trabecular network using computed tomography. Osteoporos Int 1999;9:410-9.
4. Kumasaka S, Kashima I. Initial investigation of mathematical morphology for the digital extraction of the skeletal characteristics of trabecular bone. Dentomaxillofac Radiol 1997;26:161-8.
5. Kiyohara S, Sakurai T, Kashima I. Early detection of radiation-induced structural changes in rat trabecular bone. Dentomaxillofac Radiol 2003;32:30-8.
6. Nakamura K, Matsubara M, Asai H, Koyama A, Fujikawa T, Kashima I. Mathematical morphology for extraction of bone trabecular pattern-preliminary investigation of quantitative analysis using the star volume. J Jpn Soc Bone Morphom 1999;9:45-51.
7. Ikuta A, Kumasaka S, Kashima I. Quantitative analysis using the star volume method applied to skeleton patterns extracted with a morphological filter. J Bone Miner Metab 2000;18:271-7.
8. Parkinson IH, Fazzalari NL. Methodological principles for fractal analysis of trabecular bone. J Microsc 2000;198:134-42.
9. Majumdar S, Weinstein RS, Prasad RR. Application of fractal geometry techniques to the study of trabecular bone. Med Phys 1993;20:1611-9.
10. Haidekker MA, Andresen R, Evertsz CJ, Banzer D, Peitgen HO. Assessing the degree of osteoporosis in the axial skeleton using the dependence of the fractal dimension on the grey level threshold. Br J Radiol 1997;70:586-93.
11. Cross SS. Fractals in pathology. J Pathol 1997;182:1-8.
12. Benhamou CL, Lespessailles E, Jacquet G, Harba R, Jennane R, Loussot T, et al. Fractal organization of trabecular bone images on calcaneus radiographs. J Bone Miner Res 1994;9:1909-18.
13. Majumdar S, Weinstein RS, Prasad RR. Application of fractal geometry techniques to the study of trabecular bone. Med Phys 1993;20:1611-19.
14. Majumdar S, Newitt D, Jergas M, Gies A, Chiu E, Osman D, et al. Evaluation of technical factors affecting the quantification of

trabecular bone structure using magnetic resonance imaging. Bone 1995;17:417-30.
15. Mainieri R. On the equality of Hausdorff and box counting dimensions. Chaos 1993;3:119-25.
16. Chen SK, Oviir T, Lin CH, Leu LJ, Cho BH, Hollender L. Digital imaging analysis with mathematical morphology and fractal dimension for evaluation of periapical lesions following endodontic treatment. Oral Surg Oral Med Oral Pathol Oral Radiol Endod 2005;100:467-72.
17. Landis JR, Koch GG. The measurement of observer agreement for categorical data. Biometrics 1977;33:159-74.
18. Molven O, Halse A, Fristad I, MacDonald-Jankowski D. Periapical changes following root-canal treatment observed 20-27 years postoperatively. Int Endod J 2002;35:784-90.
19. Chen SK, Hollender L. Digitizing of radiographs with a flatbed scanner. J Dent 1995;23:205-8.
20. Choël L, Last D, Duboeuf F, Seurin MJ, Lissac M, Briguet A, et al. Trabecular alveolar bone microarchitecture in the human mandible using high resolution magnetic resonance imaging. Dentomaxillofac Radiol 2004;33:177-82.
21. Chung HW, Chu CC, Underweiser M, Wehrli FW. On the fractal nature of trabecular structure. Med Phys 1994;21:1535-40.
22. Foroutan-Pour K, Dutilleul P, Smith DL. Advances in the implementation of the box-counting method of fractal dimension estimation. Appl Math Comput 1999;105:195-210.
23. Swindell W, Webb S. X-ray transmission computed tomography. In: Weeb S, editor. The physics of medical imaging. Bristol, UK: IOP; 1988. p. 98-127.

Reprint requests:

Chung-Ming Chen, PhD
Institute of Biomedical Engineering
National Taiwan University
No. 1, Sec. 4, Roosevelt Road
Taipei, Taiwan
chung@ntu.edu.tw